

LETTER • OPEN ACCESS

Environmental effects in mechanical properties of few-layer black phosphorus

To cite this article: Miriam Moreno-Moreno *et al* 2016 *2D Mater.* **3** 031007

View the [article online](#) for updates and enhancements.

You may also like

- [Room-temperature bonded silicon on insulator wafers with a dense buried oxide layer formed by annealing a deposited silicon oxidation layer and surface-activated bonding](#)
Yoshihiro Koga and Kazunari Kurita
- [Impact of environment on dynamics of exciton complexes in a \$WS_2\$ monolayer](#)
Tomasz Jakubczyk, Karol Nogajewski, Maciej R Molas *et al.*
- [Enhanced nonradiative recombination in \$Al_{1-x}Ga_xN\$ -based quantum wells thinner than the critical layer thickness determined by X-ray diffraction](#)
Shuhei Ichikawa, Mitsuru Funato and Yoichi Kawakami

2D Materials



LETTER

Environmental effects in mechanical properties of few-layer black phosphorus

OPEN ACCESS

RECEIVED

20 May 2016

REVISED

12 July 2016

ACCEPTED FOR PUBLICATION

15 July 2016

PUBLISHED

16 August 2016

Original content from this work may be used under the terms of the [Creative Commons Attribution 3.0 licence](#).

Any further distribution of this work must maintain attribution to the author(s) and the title of the work, journal citation and DOI.



Miriam Moreno-Moreno¹, Guillermo Lopez-Polin¹, Andres Castellanos-Gomez², Cristina Gomez-Navarro^{1,3} and Julio Gomez-Herrero^{1,3}

¹ Departamento de Física de la Materia Condensada, Universidad Autónoma de Madrid, E-28049, Madrid, Spain

² Instituto Madrileño Estudios Avanzados IMDEA Nanociencia, Madrid E-28049, Spain

³ Centro de Investigación de Física de la Materia Condensada (IFIMAC), Universidad Autónoma de Madrid, E-28049, Madrid, Spain

Keywords: black phosphorus, elastic modulus, nano indentations, environmental effects

Supplementary material for this article is available [online](#)

Abstract

We report on the mechanical properties of few-layer black phosphorus (BP) nanosheets, in high vacuum and as a function of time of exposure to atmospheric conditions. BP flakes with thicknesses ranging from 4 to 30 nm suspended over circular holes are characterized by nanoindentations using an atomic force microscope tip. From measurements in high vacuum an elastic modulus of 46 ± 10 GPa and breaking strength of 2.4 ± 1 GPa are estimated. Both magnitudes are independent of the thickness of the flakes. Our results show that the exposure to air has substantial influence in the mechanical response of flakes thinner than 6 nm but small effects on thicker flakes.

The recent isolation of atomically thin materials from bulk layered crystals by mechanical or chemical exfoliation [1, 2] holds promise to revolutionize the field of flexible electronics. Graphene is still by far the most studied two-dimensional crystal, however, other 2D crystals have recently gained considerable interest as they present similar mechanical performance while their electronic properties are complementary to those of graphene [3]. The lack of bandgap in graphene, for example, has motivated a surge of works on semiconducting 2D materials [4–7] which can also have a strong impact in future flexible electronics. Indeed, transition metal dichalcogenides (TMDCs) (Mo- and W- based dichalcogenides, mainly) have been recently used to fabricate flexible field effect transistors and photodetectors due to their high flexibility and high breaking strength [8–11].

TMDCs, however, present relatively slow photo-response and, because of the large bandgap of Mo- and W-based compounds, they are only suited for applications in a limited part of the visible range of the electromagnetic spectrum. A material with a direct and narrow bandgap together with fast photoresponse is needed to extend the detection range accessible with 2D materials. Recently, black phosphorus thin flakes have been isolated by mechanical exfoliation of bulk

synthetic crystals [12–16]. Bulk black phosphorus is a semiconductor with a direct bandgap of 0.35 eV with relatively high charge carrier mobilities in the order of $1000 \text{ cm}^2 \text{ V}^{-1} \text{ s}^{-1}$. Both values change with the number of layers, reaching more than 2 eV and around $1 \text{ cm}^2 \text{ V}^{-1} \text{ s}^{-1}$ respectively [17, 18] in its single layer form. Remarkably, strain provides another way of tuning electrical and optical properties [19–21]. A distinctive feature of BP is the in-plane anisotropy in its transport, optical and mechanical properties due to its puckered structure [22–24]. As examples (i) the in-plane anisotropy is around 64% for the electrical conductance (which is in the order of $10 \mu\text{S}$ for few-layer BP) [24] and (ii) the prominent electronic transport direction (armchair) is orthogonal to the prominent heat transport direction (zig-zag) [25].

A significant issue in BP is its environmental instability: BP is unstable in ambient conditions in its single- and few-layer form [26]. Specifically, the presence of moisture and oxygen in air leads to the degradation of the material due to the formation of oxidized phosphorus species [27]. While some studies have already addressed environmental effects in the electronic properties of BP [26, 28–31], little is still known about its effect on the mechanical properties.

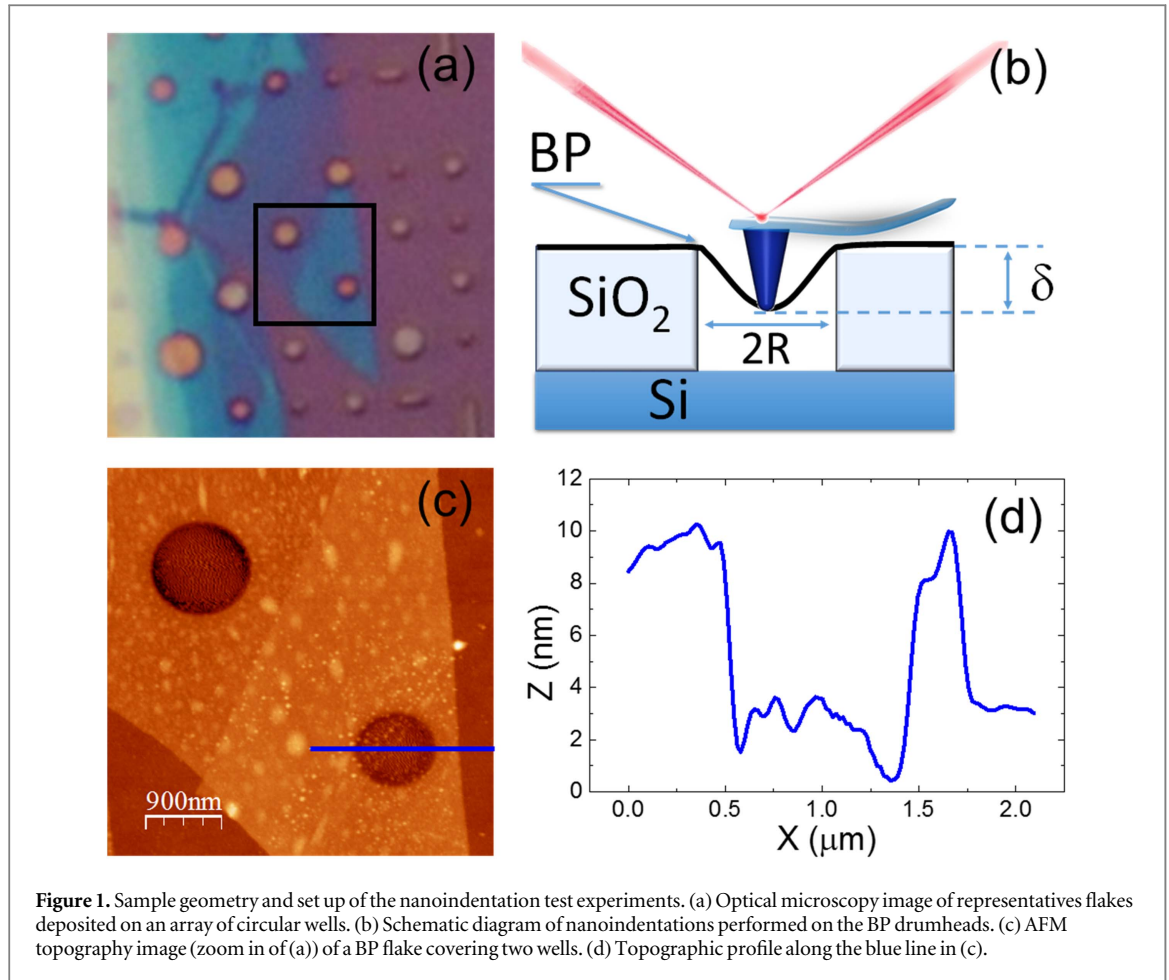


Figure 1. Sample geometry and set up of the nanoindentation test experiments. (a) Optical microscopy image of representatives flakes deposited on an array of circular wells. (b) Schematic diagram of nanoindentations performed on the BP drumheads. (c) AFM topography image (zoom in of (a)) of a BP flake covering two wells. (d) Topographic profile along the blue line in (c).

Here we investigate the role of air ambient exposition in the mechanical properties of BP. Atomic force microscopy (AFM) indentation experiments carried out in high vacuum conditions (HV, $\sim 10^{-6}$ mbar) yield elastic modulus of $E_{3D} = 46 \pm 10$ GPa for flake thicknesses ranging between 4 and 30 nm. Due to the geometry of our experiments (indentations at the center of BP circular membranes), the obtained E_{3D} is an average of the elastic modulus in both in-plane directions (zig-zag and armchair). Considering this, the measured value of E_{3D} is in good agreement with previous measurements in atmospheric conditions [24] and with theoretical predictions [32–35]. Our results also show that the exposure to air has a small effect on flakes thicker than 7 nm, even for time periods as long as 200 h, but substantial influence in the mechanical response of flakes thinner than 6 nm (corresponding to 10–12 layers).

For this study BP drumheads were prepared by mechanical exfoliation of bulk black phosphorus (smart elements) on SiO₂ (300 nm)/Si substrates with predefined circular wells with diameters ranging from 0.5 to 3 μm (figures 1(a), (c) and supplementary information 1). The mechanical properties of the membranes were tested by indenting with an AFM tip at the center of the suspended area as sketched in figure 1(b)

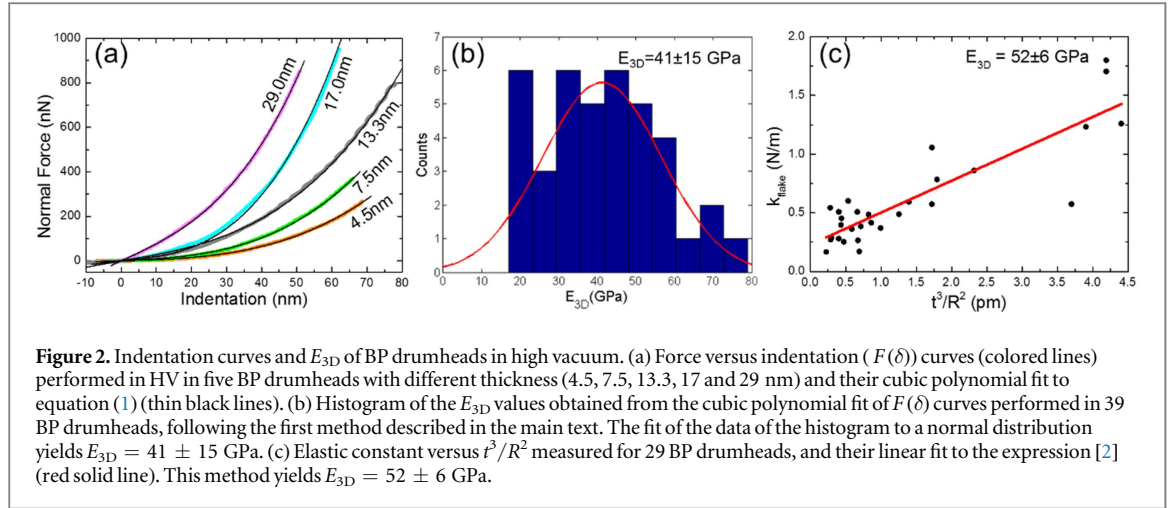
(details about the AFM probe can be found in supplementary information 2).

During the sample preparation procedure BP samples were not exposed to atmospheric conditions for more than 2 h (below this time no substantial degradation is appreciated [26]). Samples were kept and initially measured in a HV chamber. Subsequent to a complete characterization of their mechanical properties in HV conditions, a set of measurements in each membrane was performed while they were exposed to environment to assess the influence of ambient conditions in few-layer BP mechanical properties.

AFM indentation experiments on freely suspended BP can be modeled as clamped circular drumheads with central point loading (supplementary information 3). The force F versus indentation δ curves can be approximated by [9]

$$F = \left[\frac{4\pi E_{3D}}{3(1 - \nu^2)} \cdot \left(\frac{t^3}{R^2} \right) \right] \cdot \delta + \pi \sigma_0 \cdot \delta + \left(\frac{q^3 E_{3D} t}{R^2} \right) \cdot \delta^3, \quad (1)$$

where E_{3D} and ν are the elastic modulus and the Poisson's ratio respectively (the last one taken as 0.45, as the average of the Poisson's ratio in the [100] and in the [010] direction, from [34]), t is the thickness of the



nanosheet, R its radius, σ_0 the pre-tension and $q = 1/(1.05 - 0.15\nu - 0.16\nu^2)$ is a dimensionless parameter close to 1. The first term in the equation is associated with the bending rigidity and is negligible for few layered flakes. The second term, also linear in δ , accounts for the effect of small pre-stress accumulated in the membrane during the fabrication method and varies quite randomly from drumhead to drumhead. Finally, the term in δ^3 dominates at large indentations and is governed by the intrinsic elastic modulus of the sheets.

The thickness and deflection dependences reflected in equation [1] provide two complementary methods for determining E_{3D} . In the first method the experimental data of each indentation curve are fitted to a polynomial with terms in δ and δ^3 and the elastic modulus is extracted from the cubic coefficient. It requires large indentations but the value of E_{3D} can be obtained with data of exclusively one drumhead. This method automatically separates the linear coefficients from the elastic modulus, however it is not easy to apply to thick flakes where the large indentation regime is difficult to achieve. Therefore, by using this method, the elastic modulus is directly obtained from each indentation curve, however, the bending rigidity and pre-tension are not separately accessible since both contribute to the linear coefficient. The second method consists in measuring a set of flakes with different thicknesses and/or radii in the low indentation regime, where the term in δ^3 is negligible. Therefore the $\partial F/\partial \delta$ (the spring constant of each flake, k_{flake}) scales as t^3/R^2 [9]. Consequently, the elastic modulus is inferred by linear fitting of k_{flake} versus t^3/R^2 for several drumheads, according to this expression

$$k_{\text{flake}} = \left. \frac{\partial F}{\partial \delta} \right|_{\delta \approx 0} = \frac{4\pi E_{3D}}{3(1-\nu^2)} \cdot \left(\frac{t^3}{R^2} \right) + \pi \sigma_0. \quad (2)$$

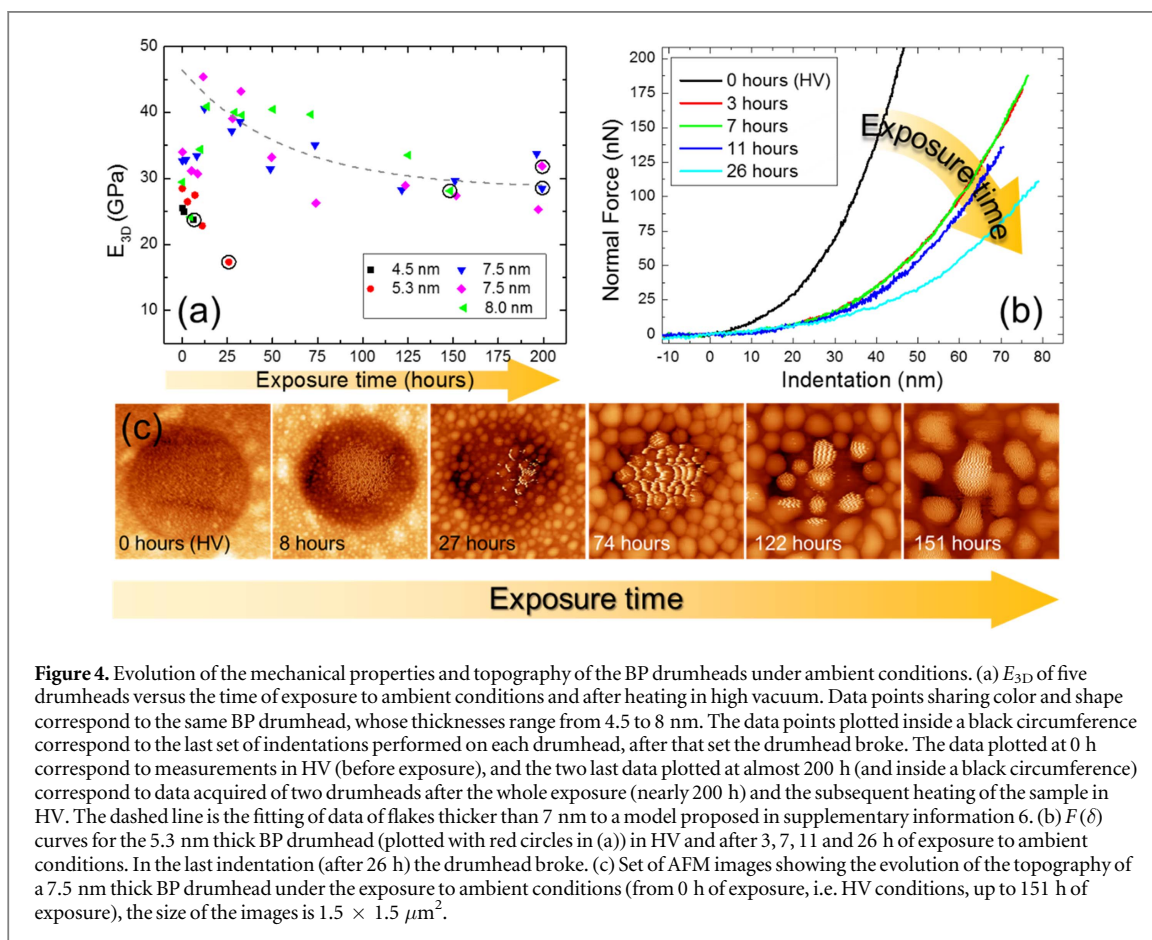
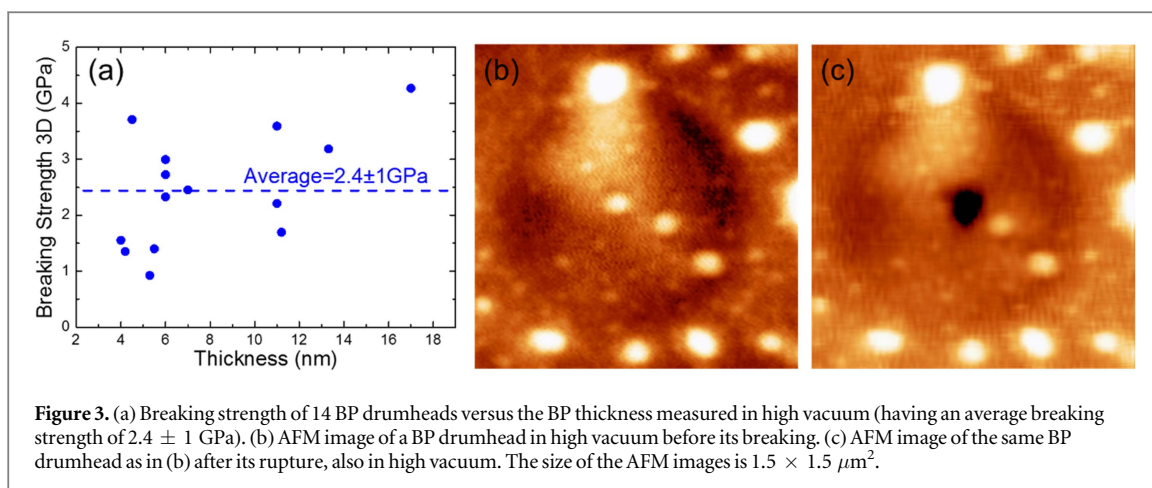
This second method is valid while the pre-tensions of all the drumheads are similar. Under that assumption, a linear fit would provide information about the Young's modulus (from the slope) and the average pre-tension of them (from the intercept).

Figure 2 summarizes our main findings in high vacuum conditions. Figure 2(a) portrays up to 5 representative indentation curves acquired on flakes with thicknesses ranging from 4.5 up to 29 nm. Figure 2(b) displays a histogram of the values obtained for the elastic modulus of 39 different flakes as obtained employing the first method aforementioned. The average value for E_{3D} is 41 ± 15 GPa, without any appreciable tendency with flake thickness. The pre-stress obtained from the linear term are in the range of 0.05 up to 0.3 N m^{-1} (obtained exclusively from flakes thinner than 5 nm where the bending rigidity is much lower than the pre-stress). Figure 2(c) depicts a set of experimental data points obtained in the low indentation regime, and it plots k_{flake} versus t^3/R^2 , following the second method described above. The obtained elastic modulus value is 52 ± 6 GPa, within the error of the elastic modulus obtained in figure 2(b), and an average pre-tension of $0.07 \pm 0.02 \text{ N m}^{-1}$.

In order to analyze the influence of random pre-tensions in the flakes (which would lead to different intercepts in the linear fit of figure 2(c)), we have numerically simulated $F(\delta)$ curves with random pre-tensions in the low indentation regime (see supplementary information 4). Here we observe that the dispersion of the simulated data is similar to that of our experiments. This suggests that the variation of pre-tension among nanosheets is the main source of noise in the experimental data.

Summarizing, both methodologies yield similar results of the elastic modulus of few layered BP, being 46 ± 10 GPa the weighted average of both values (taking into account the number of drumheads analyzed with each method).

Towards measuring the breaking strength (σ_{max}) of BP, some of the drumheads were indented until rupture. In order to estimate the strength we assume that it can be expressed as [36] $\sigma_{\text{max}} = (F_{\text{break}} E_{3D} / 4\pi R_{\text{tip}} t)^{1/2}$, where F_{break} is the rupture force and R_{tip} the tip radius. Figure 3(a) depicts a chart of the breaking strength versus thickness for 14 BP drumheads measured in high vacuum. The plot does not show any



clear correlation between these two magnitudes. The average breaking strength is found to be 2.4 ± 1 GPa. This value compares quite well with previous measurements in atmospheric conditions [24]. Figures 3(b) and (c) displays a BP membrane before and after breaking. As it can be readily seen, the crack is confined around the tip-sample contact point in contrast with other 2D materials such as MoS_2 or graphene [8, 37].

Subsequent to mechanical characterization in HV conditions, measurements in ambient atmosphere were performed. Once the samples were exposed to ambient conditions, measurements separated by

intervals of few hours were carried out in each membrane. The relative humidity was $\approx 47\%$ and the temperature $\approx 22^\circ\text{C}$. This scheme allows monitoring the evolution of E_{3D} with the exposure time to ambient conditions. For the analysis of the nanoindentation measurements at atmospheric exposure, the first method described above was used. The results obtained from these experiments are depicted in figure 4(a), which shows the evolution of E_{3D} as a function of the exposure time to atmosphere.

According to our measurements BP flakes with thickness above 7 nm show a minor reduction of its elastic modulus upon ambient conditions exposure

suggesting the growth of a passivation layer. This is readily observed in the data plotted with blue, pink and green symbols in figure 4(a). We have considered a simple passivation process (see supplementary information 6). According to this model, an exponential decay fitting of these three sets of data is depicted by a dashed line. On the other hand, flakes with thickness below 6 nm show a clear tendency of decreasing elastic modulus when exposed to air (black squares and red dots in figure 4(a)), reaching a decrease of a factor of almost two at 24 h of exposure to ambient. This fast decreasing in E_{3D} for drumheads thinner than 6 nm can be clearly appreciated in figure 4(b), which shows several indentation curves acquired at increasing exposure time in the 5.3 nm thick flake of figure 4(a). It is plain to see that the elastic modulus decreases with time in this case. Indeed, the 4.5 nm thick flake spontaneously broke after the first 10 h of exposure. Furthermore, all the flakes studied under ambient conditions, broke at forces well below forces that were previously supported.

As previously reported [26], our AFM topographic images of BP drumheads showed significant changes as a function of time of ambient exposure. Figure 4(c) displays AFM images showing the evolution of the topography of a representative BP flake with exposure time. As a consequence of water absorption we observe a random population of protrusions increasingly covering the surface. It should be noticed the difference between bubbles, that were present immediately after sample preparation, and protrusions originated by moisture. It is also worth mentioning that the fitting errors of the indentation curves also increase with time, most probably due to the presence of these protrusions, which slightly alter the shape of these curves (see supplementary information 3).

In brief: the main conclusions derived from our latter experiments are three: (i) although exposure to air leads to substantial changes in the topography of the few-layer BP, the elastic modulus of flakes thicker than 7 nm is slightly reduced, (ii) BP flakes thinner than 6 nm, experience a significant decrease of their E_{3D} upon exposure to ambient conditions, and (iii) for both thickness ranges the rupture forces seem to decrease with the ambient degradation.

The elastic modulus of the flakes upon degradation yields the magnitude $E_{3D} \cdot t = E_{2D}$. For the results plotted in figure 4, the value of thickness, t , used to derive E_{3D} is the height of the flake measured by AFM under high vacuum conditions. Upon exposure to atmosphere this magnitude becomes experimentally inaccessible for some time, i.e. the topography of the flakes reflects a growing height due to water absorption on the flakes that does not correspond to their actual thickness. Hence, the decrease of elastic modulus observed in our measurements might be ascribed to two different physical origins: (i) an inherent decrease of the E_{3D} of the material and/or (ii) a decrease of the thickness of the membrane. In order

to investigate these effects the samples were annealed in high vacuum at 230 °C during 15 h. Following previous works, under these conditions a removal of adsorbed water occurs. This allows measuring the real thickness of the flakes. According to our AFM images before and after annealing (see supplementary information 5) the change in thickness is negligible, hence suggesting that a decrease of the intrinsic elastic constants is taking place during exposure to atmospheric conditions.

This decrease in E_{3D} could be attributed to the passivation of the outer layers of the BP flakes leading to phosphorus oxide layers with a lower elastic modulus than that of pristine BP. Therefore, we consider the previously introduced passivation model (see supplementary information 6), in which the passivation layer depth increases at a rate that exponentially decreases with time, and the total thickness of the drumhead is constant in the whole process (as figure S7 in supplementary information 5 suggests). In order to draw conclusions from this model, determination of flake's thickness is paramount. As the real thickness of the flakes is now available, it is possible to complete the passivation model, which yields a maximum passivation depth of 9 ± 5 nm and a passivation characteristic time of 60 ± 20 h. The reduction factor of elastic modulus of the phosphorene oxide with respect to the one of pristine phosphorene is reported to be around 0.66 [38], leading to an elastic modulus of 30 ± 7 GPa for fully oxidized few-layer BP (46 ± 10 GPa was taken as elastic modulus of pristine few-layer BP).

According to our model, the maximum of the elastic modulus should occur at 0 h of exposure. However, the experimental results for flakes thicker than 7 nm show an increase of E_{3D} for low exposure times. This behavior was theoretically predicted for phosphorene oxide in [38] and it is rationalized in terms of small relaxations of phosphorene due to chemisorbed oxygen atoms.

The presented results are in good agreement with those published by Tao *et al* [24] of mechanical characterization in air of thick (>14 nm) flakes but in clear disagreement with a more recent publication by Wang *et al* [39].

In conclusion, in this work high vacuum measurements of BP mechanical properties are reported. Indentation experiments yield elastic modulus of 46 ± 10 GPa and breaking strength of 2.4 ± 1 GPa. The elastic modulus barely decreases in atmospheric conditions for thick flakes but we found a clear decreasing tendency for the thinnest flakes measured in our experiments. This is attributed to a self-passivation process that saturates with time.

Acknowledgments

Financial support was received from MAT2013-46753-C2-2-P that includes Miriam Moreno-

Moreno's FPI fellowship, CSD2010-0024, 'María de Maeztu' Programme for Units of Excellence in R&D (MDM-2014-0377). AC-G also acknowledges financial support from the BBVA Foundation through the fellowship 'I Convocatoria de Ayudas Fundación BBVA a Investigadores, Innovadores y Creadores Culturales' ('Semiconductores ultradelgados: hacia la optoelectrónica flexible'), from the MINECO (Ramón y Cajal 2014 program, RYC-2014-01406) and from the MICINN (MAT2014-58399-JIN). We also acknowledge MAD2D-CM, S2013/MIT-3007.

References

- [1] Novoselov K S, Jiang D, Schedin F, Booth T J, Khotkevich V V, Morozov S V and Geim A K 2005 Two-dimensional atomic crystals *Proc. Natl Acad. Sci. USA* **102** 10451–3
- [2] Coleman J N *et al* 2011 Two-dimensional nanosheets produced by liquid exfoliation of layered *Mater. Sci.* **331** 568–71
- [3] Castellanos-Gomez A, Singh V, van der Zant H S J and Steele G A 2015 Mechanics of freely-suspended ultrathin layered materials *Ann. Phys.* **527** 27–44
- [4] Koppens F H L, Mueller T, Avouris P, Ferrari A C, Vitiello M S and Polini M 2014 Photodetectors based on graphene, other two-dimensional materials and hybrid systems *Nat. Nanotechnol.* **9** 780–93
- [5] Butler S Z *et al* 2013 Progress, challenges, and opportunities in two-dimensional materials beyond graphene *ACS Nano* **7** 2898–926
- [6] Buscema M, Island J O, Groenendijk D J, Blanter S I, Steele G A, van der Zant H S J and Castellanos-Gomez A 2015 Photocurrent generation with two-dimensional van der Waals semiconductors *Chem. Soc. Rev.* **44** 3691–718
- [7] Xia F, Wang H, Xiao D, Dubey M and Ramasubramanian A 2014 Two-dimensional material nanophotonics *Nat. Photon.* **8** 899–907
- [8] Bertolazzi S, Brivio J and Kis A 2011 Stretching and breaking of ultrathin MoS₂ *ACS Nano* **5** 9703–9
- [9] Castellanos-Gomez A, Poot M, Steele G A, van der Zant H S J, Agrait N and Rubio-Bollinger G 2012 Elastic properties of freely suspended MoS₂ nanosheets *Adv. Mater.* **24** 772–5
- [10] Lee G-H *et al* 2013 Flexible and transparent MoS₂ field-effect transistors on hexagonal boron nitride-graphene heterostructures *ACS Nano* **7** 7931–6
- [11] Pu J, Yomogida Y, Liu K-K, Li L-J, Iwasa Y and Takenobu T 2012 Highly flexible MoS₂ thin-film transistors with ion gel dielectrics *Nano Lett.* **12** 4013–7
- [12] Buscema M, Groenendijk D J, Blanter S I, Steele G A, van der Zant H S J and Castellanos-Gomez A 2014 Fast and broadband photoresponse of few-layer black phosphorus field-effect transistors *Nano Lett.* **14** 3347–52
- [13] Castellanos-Gomez A 2015 Black phosphorus: narrow gap, wide applications *J. Phys. Chem. Lett.* **6** 4280–91
- [14] Churchill H H and Jarillo-Herrero P 2014 Two-dimensional crystals phosphorus joins the family *Nat. Nanotechnol.* **9** 330–1
- [15] Li L, Yu Y, Ye G J, Ge Q, Ou X, Wu H, Feng D, Chen X H and Zhang Y 2014 Black phosphorus field-effect transistors *Nat. Nanotechnol.* **9** 372–7
- [16] Ling X, Wang H, Huang S, Xia F and Dresselhaus M S 2015 The renaissance of black phosphorus *Proc. Natl Acad. Sci. USA* **112** 4523–30
- [17] Cao Y *et al* 2015 Quality heterostructures from two-dimensional crystals unstable in air by their assembly in inert atmosphere *Nano Lett.* **15** 4914–21
- [18] Liang L, Wang J, Lin W, Sumpter B G, Meunier V and Pan M 2014 Electronic bandgap and edge reconstruction in phosphorene materials *Nano Lett.* **14** 6400–6
- [19] Cakir D, Sahin H and Peeters F M 2014 Tuning of the electronic and optical properties of single-layer black phosphorus by strain *Phys. Rev. B* **90** 205421
- [20] Roldán R, Castellanos-Gomez A, Cappelluti E and Guinea F 2015 Strain engineering in semiconducting two-dimensional crystals *J. Phys.: Condens. Matter* **27** 313201
- [21] Walia S, Nili H, Balendhran S, Late D J, Sriram S and Bhaskaran M 2016 In situ characterisation of nanoscale electromechanical properties of quasi-two-dimensional MoS₂ and MoO₃ *arXiv:1409.4949*
- [22] Luo Z, Maassen J, Deng Y, Du Y, Garrelts R P, Lundstrom M S, Ye P D and Xu X 2015 Anisotropic in-plane thermal conductivity observed in few-layer black phosphorus *Nat. Commun.* **6** 8572
- [23] Qiao J, Kong X, Hu Z-X, Yang F and Ji W 2014 High-mobility transport anisotropy and linear dichroism in few-layer black phosphorus *Nat. Commun.* **5** 4475
- [24] Tao J *et al* 2015 Mechanical and electrical anisotropy of few-layer black phosphorus *ACS Nano* **9** 11362–70
- [25] Fei R, Faghaninia A, Soklaski R, Yan J-A, Lo C and Yang L 2014 Enhanced thermoelectric efficiency via orthogonal electrical and thermal conductances in phosphorene *Nano Lett.* **14** 6393–9
- [26] Island J O, Steele G A, van der Zant H S J and Castellanos-Gomez A 2015 Environmental instability of few-layer black phosphorus *2D Mater.* **2** 011002
- [27] Wood J D, Wells S A, Jariwala D, Chen K-S, Cho E, Sangwan V K, Liu X, Lauhon L J, Marks T J and Hersam M C 2014 Effective passivation of exfoliated black phosphorus transistors against ambient degradation *Nano Lett.* **14** 6964–70
- [28] Donarelli M, Ottaviano L, Giancaterini L, Fioravanti G, Perrozzi F and Cantalini C 2016 Exfoliated black phosphorus gas sensing properties at room temperature *2D Mater.* **3** 025002
- [29] Erande M B, Pawar M S and Late D J 2016 Humidity sensing and photodetection behavior of electrochemically exfoliated atomically thin-layered black phosphorus nanosheets *ACS Appl. Mater. Interfaces* **8** 11548–56
- [30] Late D J 2016 Liquid exfoliation of black phosphorus nanosheets and its application as humidity sensor *Microporous Mesoporous Mater.* **225** 494–503
- [31] Wang Z, Islam A, Yang R, Zheng X and Feng P X-L 2015 Environmental, thermal, and electrical susceptibility of black phosphorus field effect transistors *J. Vac. Sci. Technol. B* **33** 052202
- [32] Appalakondaiah S, Vaitheeswaran G, Lebègue S, Christensen N E and Svane A 2012 Effect of van der Waals interactions on the structural and elastic properties of black phosphorus *Phys. Rev. B* **86** 035105
- [33] Jiang J-W and Park H S 2014 Mechanical properties of single-layer black phosphorus *J. Phys. D: Appl. Phys.* **47** 385304
- [34] Wei Q and Peng X 2014 Superior mechanical flexibility of phosphorene and few-layer black phosphorus *Appl. Phys. Lett.* **104** 251915
- [35] Yang Z, Zhao J and Wei N 2015 Temperature-dependent mechanical properties of monolayer black phosphorus by molecular dynamics simulations *Appl. Phys. Lett.* **107** 023107
- [36] Lee C, Wei X, Kysar J W and Hone J 2008 Measurement of the elastic properties and intrinsic strength of monolayer graphene *Science* **321** 385–8
- [37] Lopez-Polin G, Gomez-Herrero J and Gomez-Navarro C 2015 Confining crack propagation in defective graphene *Nano Lett.* **15** 2050–4
- [38] Hao F and Chen X 2015 Mechanical properties of phosphorene nanoribbons and oxides *J. Appl. Phys.* **118** 234304
- [39] Jia-Ying Wang Y L, Zhan Z-Y, Li T, Zhen L and Xu C-Y 2016 Elastic properties of suspended black phosphorus nanosheets *Appl. Phys. Lett.* **108** 013104